Review

Progress in *Henipavirus* Neutralizing Antibody for Therapeutic Development

Junping Hong [1,2], Yuanteng Zhao [1,2], Ethan H. Zhou [3], Eleni Kourlas [1,2], Zhangfei Shen [1,2], and Kai Xu [1,2,4,*]

[1] Center for Retrovirus Research, The Ohio State University, Columbus, OH 43210, USA
[2] Department of Veterinary Biosciences, The Ohio State University, Columbus, OH 43210, USA
[3] Bullis School, Potomac, MD 20854, USA
[4] Department of Microbial Infection and Immunity, The Ohio State University, Columbus, OH 43210, USA
* Correspondence: xu.4692@osu.edu
Received: 8 August 2025; Revised: 15 October 2025; Accepted: 28 October 2025; Published: 22 January 2026

Abstract: Henipaviruses are lethal zoonotic paramyxoviruses with high mortality, increasing geographic reach, and a growing number of identified species and variants. No vaccines or therapeutics are licensed for human use, creating an urgent need for effective interventions. This review highlights recent advances in neutralizing antibodies against the viral attachment (G) and fusion (F) glycoproteins, focusing on structural and mechanistic insights. Lead monoclonal antibodies target conserved epitopes and block viral entry through receptor interference or fusion inhibition. Key challenges, including narrow treatment windows and viral escape, underscore the need for rationally designed combinations and broad-spectrum, escape-resistant candidates. By consolidating current progress, we outline strategies for developing antibody therapeutics with high translational impact, serving as a first line of defense in outbreak settings and as a complementary intervention to vaccines for comprehensive henipavirus management.

Keywords: henipavirus; antibody; structure

1. Introduction

Henipaviruses are negative-sense, single-stranded RNA viruses of the *Paramyxoviridae* family [1]. They are enveloped and pleomorphic, ranging from ~40 to 1900 nm in size, and appear spherical or filamentous under electron microscopy [2]. Their 18.2 kb genomes, among the largest in the family [3,4], encode six structural proteins: nucleocapsid (N), phosphoprotein (P), matrix (M), fusion (F), attachment (G), and large polymerase (L). The P gene also produces accessory proteins (V, W, and C), although their expression varies among species (Figure 1A). Viral RNA, together with N, P, and L, forms the ribonucleoprotein (RNP) complex that drives replication and transcription (Figure 1B) [5].

While some taxonomic classifications distinguish between *Henipavirus* and *paraHenipavirus* genera [6], for simplicity and broader applicability, this review refers to all related viruses collectively as *Henipavirus* unless otherwise specified.

The first identified *Henipavirus* was *Hendra virus (*HeV), also known as equine morbillivirus. HeV was first discovered in 1994 in the Brisbane suburb of Hendra, Australia (Figure 2) [7,8]. In 1998–1999, *Nipah virus* (NiV) was recognized during outbreaks in Malaysia and Singapore; it was later named after Kampung Sungai Nipah in Malaysia [9–11]. Since 2001, NiV has caused nearly annual outbreaks in Bangladesh and India, resulting in hundreds of human cases [12]. Ghana virus (GhV) was reported in 2008 from fruit bats in Ghana, followed by *Cedar virus* (CedV) in 2009 from fruit bats in Australia [13,14]. *Mojiang virus* (MojV) was discovered in 2012 following the deaths of three miners from severe pneumonia in Yunnan Province, China [15]. Between 2017 and 2021, two bat-borne viruses, Yunnan bat henipavirus 1 and 2, were identified from bat kidney tissues in China, showing close evolutionary relationships to NiV and HeV [16]. In 2021, Daeryong virus and Gamak virus were reported from South Korea [17], while Wenzhou virus, Jingmen virus, and Wufeng virus were detected in China [18]. That same year, a new HeV variant, HeV genotype 2 (HeV-g2), was detected in Australia [19], and Camp Hill virus (CHV) was identified in northern short-tailed shrews (*Blarina brevicauda*) in Alabama, USA, marking the first documented henipavirus in North America [20]. In 2022, several additional henipaviruses were reported:

Peixe-Bol virus from Brazil, Denwin virus from Belgium, Melian virus from Guinea, Angavokely virus from Madagascar, and *Langya virus* (LayV) from eastern China through zoonotic disease surveillance efforts [21–24]. Among these viruses, only HeV, NiV, LayV, and MojV have been linked to human disease.

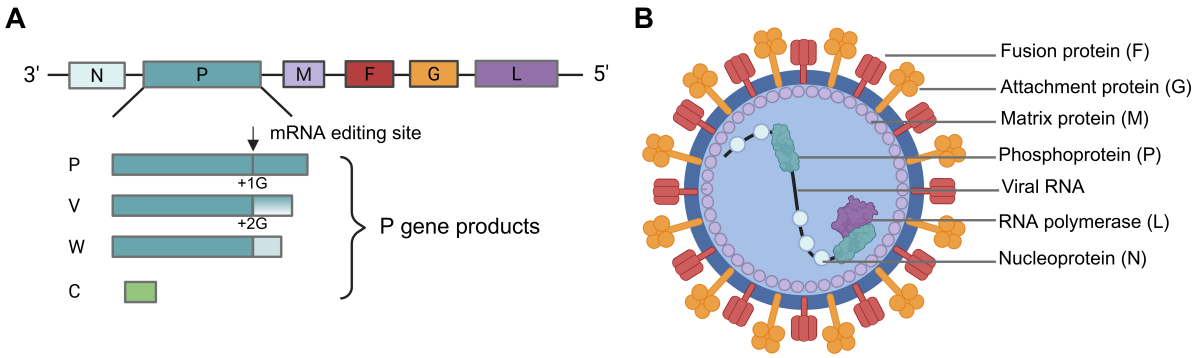

Figure 1. Schematic representation of the Henipavirus genome organization and the viral structure. (**A**) The henipavirus genome consists of a single-stranded, negative-sense RNA encoding six structural proteins: nucleoprotein (N), phosphoprotein (P), matrix protein (M), fusion protein (F), attachment glycoprotein (G), and RNA-dependent RNA polymerase (L). The P gene also encodes three nonstructural proteins: V and W (produced via mRNA editing by insertion of one or two guanosine residues, respectively) and C (translated from an alternative open reading frame). (**B**) The pleomorphic viral particle contains a ribonucleoprotein (RNP) core (composed of N, P, and L proteins bound to viral RNA) surrounded by a host-derived lipid envelope embedded with F and G glycoproteins. The M protein lines the inner surface of the envelope. Created with BioRender.com.

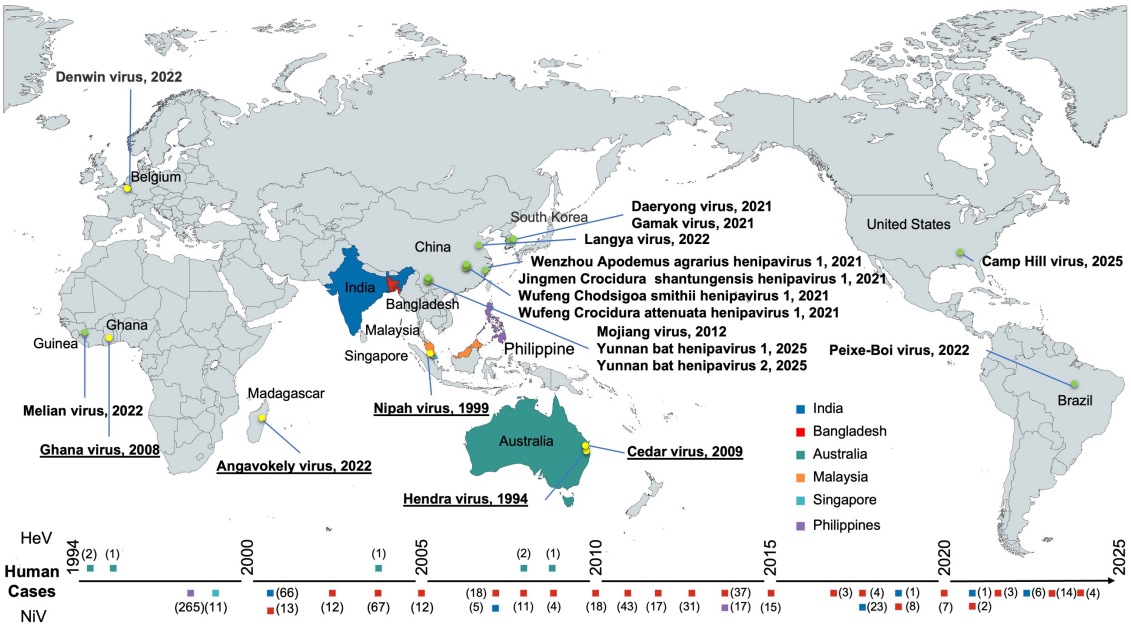

Figure 2. Global distribution of henipaviruses: Discovery locations and human outbreaks. Yellow circles indicate five classified henipavirus species (HeV, NiV, GhV, CedV and AngV), labeled with virus names and year of first report or GenBank submission (underlined). Light green circles represent additional henipavirus species, also labeled accordingly. The bottom panel shows a timeline of reported human cases of HeV and NiV outbreaks, annotated with case numbers in parentheses. Countries are color-coded as follows: dark blue (India), red (Bangladesh), dark green (Australia), orange (Malaysia), light green (Singapore), and purple (Philippines). Figure created using mapchart.net.

Fruit bats (*Pteropodidae*), particularly species within the *Pteropus* genus, constitute the principal natural reservoirs of henipaviruses (Figure 3) [25]. These volant mammals sustain viral circulation across broad geographic regions, and their sympatry with densely populated human areas facilitates zoonotic spillover. Henipaviruses are shed via multiple excreta and secretions [26], leading to environmental contamination. Cross-species transmission is initiated when intermediate hosts encounter these contaminated materials. For HeV, horses serve as the primary

bridge species [7,8], while NiV utilizes porcine intermediaries in the Malaysian strain (NiV-M) [27]. The Bangladesh strain (NiV-B) demonstrates increased capacity for direct bat-to-human transmission [28]. Human-to-human transmission has been documented for NiV, predominantly NiV-B, but remains unreported for HeV [29].

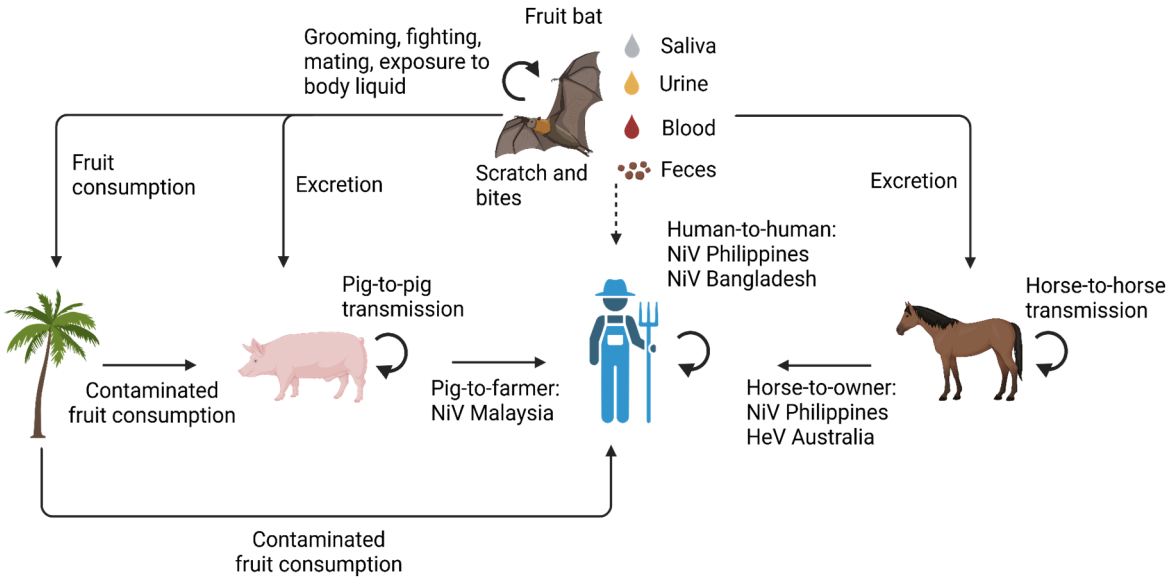

Figure 3. Transmission cycles of HeV and NiV: Zoonotic spillover from fruit bats to humans. This diagram illustrates the transmission dynamics of henipaviruses from their natural reservoir (fruit bats) to humans. Fruit bats shed the virus through multiple bodily fluids (saliva, urine, blood, feces) during activities such as grooming, fighting, and mating. Primary spillover events arise via (1) consumption of virus-contaminated fruit by intermediate hosts or humans, (2) direct exposure to bats via scratches and bites, and (3) viral excretion routes. Secondary transmission has been documented in multiple pathways: pig-to-pig transmission; pig-to-farmer (NiV in Malaysia); human-to-human (NiV in Philippines and NiV in Bangladesh); horse-to-horse transmission; and horse-to-owner (NiV in Philippines, HeV in Australia). The circular arrows indicate transmission within species. Created with BioRender.com.

HeV and NiV infections exhibit a wide clinical spectrum, ranging from asymptomatic (subclinical) cases to rapidly progressive, life-threatening illnesses. Following exposure, symptoms typically manifest within two weeks in over 90% of cases, though incubation periods extending to two months have been documented [30]. The clinical manifestations commonly begin as acute febrile illness characterized by flu-like symptoms such as fever, myalgia, sore throat, and dizziness, which may rapidly progress to severe encephalitic and/or respiratory syndromes [31,32]. Both HeV and NiV are classified as biosafety level 4 agents due to their high pathogenicity, lack of approved therapeutics, and potential human-to-human transmission. Case fatality rates range from 70% to 100% depending on outbreak location and healthcare capacity [33].

Henipavirus entry into host cells is mediated by two essential envelope glycoproteins: the attachment glycoprotein G and the fusion glycoprotein F (Figure 1). The G protein is a type II single-pass transmembrane protein composed of an N-terminal cytoplasmic tail, an extended a-helical stalk region, and a C-terminal six-blade β-propeller head domain responsible for receptor binding. Oligomerization of G proteins is driven by the stalk region, where intermonomer disulfide bonds facilitate the formation of a stable tetrameric structure through a "dimer of dimers" assembly mechanism [34,35]. Unlike other paramyxoviral attachment proteins, the henipavirus G protein lacks both hemagglutinating and neuraminidase activities [7,8,10]. G specifically mediates attachment to host cell surface receptors, such as ephrin B2/B3 receptors (Table 1). The non-pathogenic CedV has a broader receptor usage, including ephrin B1 and ephrin A2/A5, but A2 and A5 have weak interactions. CedV G protein also binds to mouse A1 but not human A1 (Table 1) [36]. The F protein is a class I viral fusion glycoprotein and a type I transmembrane protein with a C-terminal cytoplasmic domain. It is initially synthesized as an inactive precursor (F0), which oligomerizes into a trimeric complex and is subsequently cleaved by endosomal cathepsin L or B into the functional subunits F1 and F2 [37–39]. The F1 subunit harbors key structural features necessary for membrane fusion, including a hydrophobic fusion peptide and two heptad repeat regions (HR1 and HR2), which undergo extensive conformational rearrangements to drive fusion of viral and host membranes [40,41].

The G and F glycoproteins act in concert to mediate viral attachment and membrane fusion, with the G protein serving as the primary determinant of host and tissue tropism. Upon binding to receptors, such as ephrin-B2, the G

protein undergoes conformational changes that are believed to facilitate viral entry [42]. The G protein is thought to trigger the activation of the metastable, trimeric F protein, which initiates a cascade of conformational changes [43,44], although the precise mechanism remains incompletely understood. The F protein transitions into an extended pre-hairpin intermediate upon G-mediated activation, exposing its hydrophobic fusion peptide at the membrane-distal end (Figure 4) [45]. These intermediate bridges the viral and host membranes, enabling the fusion peptide to insert into the target cell membrane. The F protein then undergoes further refolding, bringing HR1 and HR2 regions together to form a stable six-helix bundle (6HB). This dramatic structural rearrangement drive membrane merger, and fusion pore formation, allowing release of the viral genome into the host cytoplasm for replication.

Table 1. Binding affinity of henipavirus G protein and Ephrin receptors.

	Ephrin-A			Ephrin-B			
	A1	**A2**	**A5**	**B1**	**B2**	**B3**	**Ref.**
NiV	24.5 nM (Mouse)	196.0 nM	113.0 nM	0.24 nM	0.11 nM	2.83 nM	[46]
HeV					17.3 nM	Binding	[47]
CedV					0.56 nM	No Binding	[36]
GhV					Binding	No Binding	[48,49]
MojV					No Binding	No Binding	[35,49]
LayV					No Binding	No Binding	[35,50]

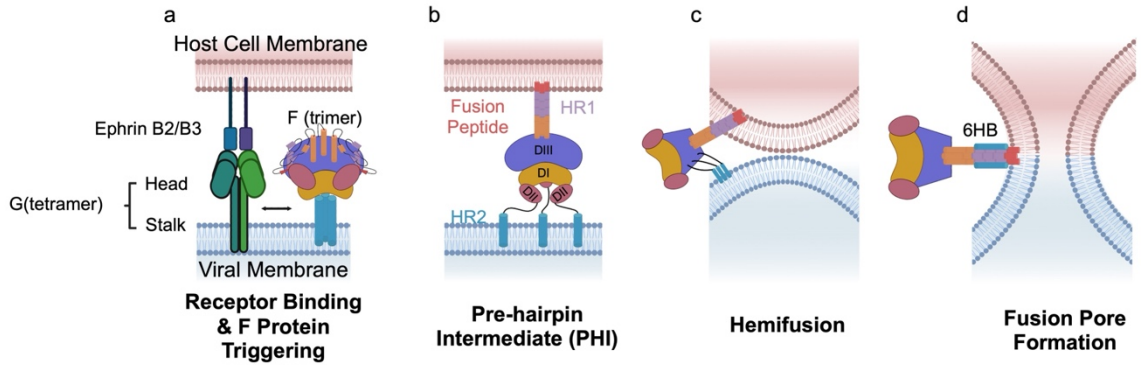

Figure 4. Henipavirus membrane fusion and viral entry cascade. The membrane fusion cascade is depicted in three sequential stages. (**a**) Initial receptor binding and F protein triggering: Ephrin B2 or Ephrin B3 binding to henipavirus G protein triggers the F protein through allosteric mechanisms. (**b**) Formation of the pre-hairpin intermediate (PHI): Following activation, F undergoes conformational change, extending to insert its fusion peptide into the host cell membrane. (**c**,**d**) Six-helix bundle (6HB) formation: the HR1 and HR2 regions in the PHI coalesce to form the 6HB conformation, bringing viral and cellular membranes together to facilitate fusion and viral entry. Created with BioRender.com.

The G and F proteins of henipaviruses play critical roles in viral entry, making them prime targets for vaccine and antibody-based therapeutic development. Although no FDA-approved vaccines or therapeutics currently exist, several candidates have advanced to clinical trials. Three vaccine candidates have progressed to clinical trials in the United States: HeV-sG-V (NCT04199169), a recombinant subunit vaccine developed by Auro Vaccines LLC containing the soluble G glycoprotein of HeV, which entered Phase 1 clinical trials in March 2020 and uses the same immunogen as Equivac® HeV, a fully registered horse anti-HeV subunit vaccine in Australia [51–53]; PHV02 (NCT06221813), a live, attenuated recombinant vesicular stomatitis virus vector vaccine expressing the glycoprotein of NiV-B; and mRNA-1215 (NCT05398796), an mRNA vaccine encoding both NiV F and G glycoproteins. The most clinically advanced henipavirus therapeutic to date is m102.4, a human monoclonal antibody (mAb) targeting the G glycoprotein, which successfully completed a Phase I clinical trial (ACTRN12615000395538) in Australia, demonstrating safety and tolerability in healthy adults with no immunogenic response [54]. m102.4 has also been approved for emergency post-exposure prophylaxis. Alongside these clinical efforts, extensive preclinical research continues to explore new antibody-based countermeasures against henipaviruses. HeV and NiV are the only henipaviruses conclusively proven to cause severe disease and high mortality in humans, establishing them as the most immediate public health threat within this genus. These two viruses also serve as the primary models for

understanding henipavirus pathogenicity and immunology. The vast majority of mechanistic studies, structural data, and *in vivo* efficacy testing have been performed using these two viruses, providing a strong foundation for comparison. Thus, this review focuses on HeV- and NiV-specific neutralizing antibodies. The fusion (F) and attachment (G) glycoproteins of NiV and HeV share approximately 88% and 83% amino acid sequence identity, respectively, and both viruses utilize the same cellular entry receptors: ephrin B2 and ephrin B3 [4,55]. This high degree conservation, particularly within structurally critical domains such as the receptor-binding site on the G protein and the fusion peptide and heptad repeat regions on the F protein, creates shared antigenic surfaces. In the following section, we summarize published antibodies against HeV and NiV, categorizing them by target epitope, neutralization mechanism, and developmental stage. Finally, we discuss translational challenges and emerging opportunities aimed at advancing broadly protective therapeutics against henipavirus.

2. Anti-G Neutralizing Antibodies

2.1. m102.4 (Human)

The human mAb m102, initially isolated from a naïve human Fab phage-displayed library using HeV G glycoprotein as the panning antigen, demonstrated cross-neutralization against both Hendra (HeV) and Nipah (NiV) viruses [56]. Subsequent affinity maturation via light chain shuffling and heavy chain random mutagenesis through error-prone PCR yielded m102.4, a high-affinity variant with most mutations localized in its heavy chain variable domain [57]. Despite being selected against HeV G, m102.4 exhibited slightly stronger binding and Ephrin B2 receptor blocking for NiV G. Both Fab and IgG formats of m102.4 showed potent cell-fusion inhibition, surpassing its parental antibody, m102. As an IgG1, m102.4 neutralized infectious NiV and HeV with half-maximal inhibitory concentration (IC50) values of <40 ng/mL and <600 ng/mL, respectively, and maintained plasma stability for ≥8 days, marking it as the first fully human antibody with high neutralization efficacy against both henipaviruses [57].

The ferret model mimicking human multisystemic vasculitis demonstrated that m102.4 provided protection even 10 h post-lethal NiV challenge (Table 2) [58]. Further studies in African green monkey (AGM) models, which closely replicate human clinical symptoms, confirmed m102.4's pharmacokinetics and efficacy against HeV (Table 2) [59–61]. Administered intravenously, m102.4 had a ~1-day distribution half-life and an ~11-day elimination half-life. Although it did not prevent viral dissemination, it significantly reduced viral loads, allowing AGMs time to develop protective immunity. Notably, m102.4-treated animals produced anti-F antibodies, unlike untreated controls.

Previous studies demonstrated that m102.4 provided complete protection against NiV in ferrets and HeV in AGMs when administered immediately post-exposure. However, clinical implementation faces challenges due to treatment delays and early disease presentation. A time-course evaluation of m102.4 efficacy in AGMs was conducted, administering a lower dose (~15 mg/kg) at 1, 3, or 5 days post-exposure, including after clinical onset (Table 2) [62]. Consistent with prior findings [61], all antibody-treated groups showed circulating anti-NiV F antibodies absent in controls, suggesting host immune involvement in protection. While all m102.4-treated AGMs survived infection, controls uniformly succumbed. Subsequent research using NiV-B revealed a narrower therapeutic window for m102.4 despite comparable *in vitro* neutralization of both strains [63]. AGMs treated at day 5 and 7 post-infection failed to survive this more pathogenic variant and exhibited limited anti-F seroconversion.

m102.4 has been used compassionately as post-exposure prophylaxis in 14 high-risk individuals exposed to HeV (13 in Australia) or NiV (one in the USA) [54]. Currently the most advanced in development, m102.4 is the only NiV-targeting mAb with published Phase 1 trial data. The study, conducted in Australia, involved 40 healthy adults receiving either single escalating doses (1–20 mg/kg), two 20 mg/kg doses 72 h apart, or a placebo. No severe adverse effects—apart from mild headaches—were reported. Serum analysis confirmed m102.4 retained neutralizing activity against HeV and NiV for at least eight days without triggering an immune response. The trial demonstrated its safety and tolerability, supporting its potential as a post-exposure prophylactic against henipaviruses.

To characterize the binding epitope and neutralizing mechanism of m102.4, the crystal structure of the HeV G glycoprotein globular head domain in complex with m102.3, a variant of m102.4, was resolved [64]. The structure revealed that m102.3 binds the receptor-binding surface of HeV G in a high-affinity lock-and-key manner without inducing conformational changes, consistent with its receptor-blocking activity (Figure 5A) [56,57]. In contrast, Ephrin binding triggers major conformational rearrangements in henipavirus G protein, driving F-protein refolding and membrane fusion [47,65]. Although m102 was raised against HeV-G, it exhibits a higher affinity for NiV G (KD: 5.56 nM vs. 27.4 nM for HeV G). Structural analysis indicated that hydrophobic substitutions in NiV G (V507 and F458), which replace the corresponding HeV G residues (T507 and Y458), strengthen m102.3 binding. Intriguingly, escape mutations—V507I in NiV G and D582N in HeV G—confer resistance to neutralization by both m102.3 and m102.4, underscoring the critical role of residue V507 in m102.4 binding [64].

Table 2. *In vivo* efficacy of henipavirus-neutralizing antibodies.

Ab	Target	Species	Animal Model or Clinical Trial	Year	Dose	Strain	Result	Ref.
m102.4	G	Human	Ferret	2009	50 mg	NiV-M	Full protection in the 10 h post-challenge group. Only one ferret survived in the pre-challenge group.	[58]
m102.4	G	Human	AGM	2011	~20mg/kg, 2 doses	HeV	All AGMs treated with m102.4 survived the infection, whereas the control group did not by day 8 post-infection. Anti-F antibodies were detected in sera, confirming the role of the host immune response in protection against viral challenge. Although animals in the 72-h treatment group showed neurological symptoms, all began recovering by day 16 post-infection.	[61]
m102.4	G	Human	AGM	2014	~15mg/kg, 2 doses	NiV-M	The first dose of m102.4 was delivered to AGMs at multiple time points (1, 3, or 5 days and 2 days later after the virus challenge). All antibody-treated subjects survived infection, but the control group succumbed to diseases.	[62]
m102.4	G	Human	AGM	2016	~15mg/kg, 2 dose	NiV-B	The therapeutic window for m102.4 was much shorter in NiV-B infected AGMs compared to that in NiV-M infected AGMs.	[63]
m102.4	G	Human	Phase 1 Clinical Trial	2020	1 dose: 1, 3, 10 or 20 mg/kg; 2 doses: 20 mg/kg		Administration of both single and repeated doses of m102.4 was well tolerated and safe, showing linear pharmacokinetics without any indication of an immune response.	[54]
HENV-26 and HENV-32	G	Human	Ferret	2020	15 mg/kg, 2 doses	NiV-B	Both antibodies protected ferrets from lethal virus infection. Circulating viral genomes were detected from HENV-26 treated subjects.	[66]
HENV-103 and HENV-117	G	Human	Hamster	2021	~10 mg/kg	NiV-B	Antibody cocktail guaranteed complete protection compared to partial protection by monotherapy.	[67]
41-6	G	Human	Hamster	2024	~3mg/kg or ~10mg/kg	NiV-M	41-6 provided complete protection or 67% improved survival as a prophylactic with different dosage. In the post-infection model, 41-6 provide 50% to 83% protection with different dosage and different infusion time.	[68]
1E5	G	Macaque	Hamster	2024	~4.5 mg/kg or 10 mg/kg	NiV-M	Antibodies targeting different epitopes effectively protect against lethal virus challenges. 1E5 provided full protection in pre- and post-exposure protective models.	[69]
n425	G	Human	Mouse	2024	5 mg/kg	NiV-M pseudoviruses	Both conventional IgG and n425 effectively eliminated the virus in the thoracic region, while only n425 and its smaller variant can effectively clear the virus in the brain.	[70]

Table 2. *Cont.*

Ab	Target	Species	Animal Model or Clinical Trial	Year	Dose	Strain	Result	Ref.
Anti-NiV G: Nip GIP 1.7, Nip 3B10; Anti-NiV F: Nip GIP 35, Nip GIP 3	G & F	Mouse	Hamster	2005	1.2~520 μg	NiV	Administering just 1.2 μg of anti-G mAb was sufficient to protect the animals, while a dosage exceeding 1.8 μg of anti-F MAb was necessary to achieve full protection in the pre-exposure hamster model. Anti-F antibody performed better than the anti-G antibody in the post-exposure model.	[71]
h5B3.1	F	Humanized Murine antibody	Ferret	2020	20 mg/kg, 2 doses	HeV and NiV-M	All ferrets treated with h5B3.1 survived the infection, while untreated control animals succumbed to the disease. The treated animals showed minimal to no signs of disease, contrasting with the severe symptoms and pathology observed in the control group.	[72]
mAb92	F	Rabbit	Hamster	2024	500 μg	HeV and NiV-M	mAb 92 can completely protect against the lethal NiV challenge. While mAb 92 may delay the onset of HeV infection, it ultimately failed to prevent the hamster's death.	[73]
hu1F5, hu12B2	F	Humanized murine antibody	Hamster	2024	5 mg/kg	NiV-B	hu1F5 provided complete protection. 60% of animals treated with hu12B2 survived. 80% treated with antibody cocktail (hu1F5 + hu12B2) survived the lethal virus challenge.	[74]
hu1F5	F	Humanized murine antibody	AGM	2024	25 mg/kg, 10mg/kg	NiV-B	100% of hu1F5 treated AGMs survived but only one of six animals infused with m102.4 survived. hu1F5 treated animals showed minimal clinical disease symptoms. hu1F5 retained protection efficacy with a reduced dose (10mg/kg). The development of MPB1F5 has progressed to a Phase 1 first-in-human clinical trial.	[74]
1D6, 5C8 and 5H1	F	Macaque	Hamster	2025	10 mg/kg	NiV-M	For prophylactic use, 1D6 and 5H1 provided complete protection, while 5C8 had one infection-related death. For therapeutic use, 1D6 showed an 83.3% survival rate, whereas 5H1 and 5C8 both had 66.7% survival—though 5H1 prolonged average survival to 12 days compared to 7 days by 5C8.	[75]
DS90-m102.4	F&G	Alpaca & Human	Hamster	2025	10 mg/kg	NiV-M	Prophylactically, both DS90-Fc and DS90-m102.4 provided 100% protection, whereas DS90-FcM showed no survival benefit over control mAb. The benchmark antibodies 5B3 and m102.4 conferred 83% protection. Therapeutically, DS90-Fc dimer and DS90-m102.4 achieved 50% survival against NiV-M infection, while 5B3 and m102.4 only reached ~17% survivability.	[76]

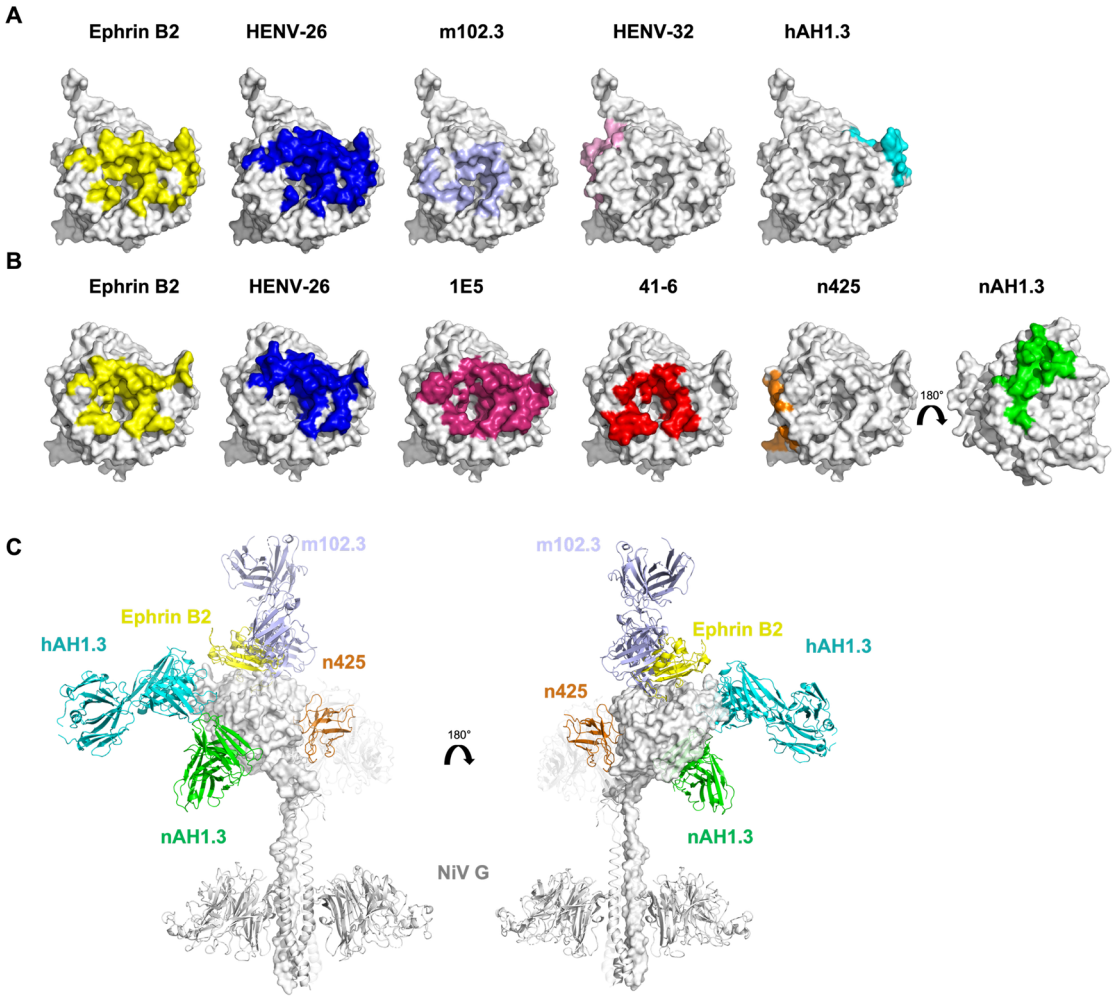

Figure 5. Epitope mapping of neutralizing antibodies targeting henipavirus G glycoproteins. (**A**) Surface representation of the Hendra virus (HeV) G head domain (PDB: 6PD4) showing the binding footprints of the ephrin-B2 receptor (yellow) and neutralizing antibodies HENV-26 (blue), m102.3 (light blue), HENV-32 (pink), and hAH1.3 (cyan). (**B**) Surface representation of the Nipah virus (NiV) G head domain (PDB: 3D11) showing the binding footprints of the ephrin-B2 receptor (yellow) and neutralizing antibodies HENV-26 (blue), 1E5 (warm pink), 41-6 (red), n425 (orange), and nAH1.3 (green). (**C**) Cartoon representation of representative neutralizing antibodies bound to the tetrameric NiV G protein (PDB: 7TXZ and 7TY0). One protomer is displayed as a surface representation, with the antibody complex modeled onto the structure.

2.2. 41-6 (Human)

In addition to m102, two neutralizing antibodies, NiV41 and NiV42, targeting the NiV G protein were also isolated from a naïve human phage-displayed Fab library [68]. NiV41 cross-reacted with both HeV and NiV G proteins, while NiV42 bound significantly stronger to NiV G than HeV G. Both antibodies prevent G protein binding to cell-surface receptors and cross-neutralize HeV and NiV in pseudovirus and authentic virus assays. In a preliminary study, NiV41 provided complete protection against chronic NiV-B infection in hamsters.

Affinity maturation through light-chain shuffling generated improved variants: NiV41-derived antibodies gained enhanced cross-neutralizing potency against both viruses, while NiV42-derived antibodies retained strong binding to NiV G but bound only weakly to HeV G, compared to the parental NiV42 antibody. Immunogenetic analysis revealed the mature antibody 42–27's light chain maintained 100% germline gene identity, while antibody 41-6 exhibited more somatic hypermutations, potentially contributing to its broader cross-reactivity.

In acute infection hamster models, 10 mg/kg of mAb 41-6 administered pre-NiV-M challenge provided complete protection, with 67% survival at reduced 3 mg/kg dosage (Table 2). Post-infection models showed 50–83% protection. The mAb 41-6 epitope is highly conserved in both NiV and HeV G proteins, explaining its cross-neutralization capability. Structural comparison between NiV G bound to mAb 41-6 and Ephrin-B2 showed considerable binding site similarity (Figure 5B), indicating mAb 41-6 mimics receptor binding to NiV G protein.

2.3. n425 (Human)

The broadly neutralizing antibody, n425 (a fully human single-domain antibody), was isolated from a fully human single-domain antibodies library through sequential screening using HeV G and NiV G proteins [70]. Competition assays showed n425 moderately competed with HENV-32 but not with four other antibodies (m102.4, HENV-26, nAH1.3, and hAH1.3). n425 demonstrated cross-neutralization against HeV, NiV-B, and NiV-M, with a combination of n425 and m102.4 showing synergistic potency.

Cryo-EM structures of n425 complexed with NiV-M G and NiV-B G (S76C) revealed that its broad neutralization stems from the conservation of epitope sequences and structure across different strains (Figure 5B). The antigenic site of n425 differs from Ephrin B2-competing antibodies like m102.4 and HENV-26, consistent with binding competition results. n425 showed superior efficacy in inhibiting cell-cell fusion and syncytium formation compared to m102.4, both as a monovalent single-domain antibody and as a bivalent Fc fusion protein.

Mechanistically, n425 binds to the inner side of NiV G tetramer (Figure 5C), locking the complex in a conformation with all four heads positioned upwards, which disrupts G tetramerization and interferes with F-induced fusion triggering. In a mouse model of NiV brain infection, n425 and its variant n425-sFc-n425 (a bivalent construct linked via an engineered single-chain Fc) exhibit superior viral clearance in the brain compared to conventional IgG antibody, m102.4, likely attributable to their smaller size, which faciliates improved tissue penetration (Table 2).

2.4. HENV-26 and HENV-32 (Human)

While the phage library-derived antibody provides valuable insights into henipavirus neutralization, naturally occurring human monoclonal antibodies (mAbs) isolated from peripheral blood mononuclear cells (PBMCs) offer additional perspectives on the native immune response. Anti-HeV G human mAbs from an individual exposed to the Equivac HeV vaccine were screened, identifying 10 mAbs with G-specificity and 9 unique antibody variable gene sequences [66]. Four antibodies cross-reacted with NiV G. All the antibodies neutralized HeV infections, with 9 of them showing the IC_{50} values below 0.78 μg/mL. Five neutralized NiV-B and seven neutralized NiV-M. The most potent antibodies, HENV-26 and HENV-32, demonstrated nanomolar affinity against both HeV and NiV G proteins. Competition-binding assays defined five antigenic regions on the HeV G head domain, with HENV-26 and HENV-32 recognizing different regions. Only HENV-26 inhibited HeV G binding to Ephrin B2 receptor in both recombinant and cell-based studies. Crystallographic analysis revealed HENV-26's epitope overlapped with receptor binding sites on both HeV and NiV G (Figure 5A,B), explaining its receptor-blocking activity. HENV-26 neutralized viral infection by inhibiting G-Ephrin B2 interaction. HENV-32's structure showed a different antigenic site from HENV-26, intersecting with the dimeric interface of the HeV-RBP head domain at the N-terminal region, which is similar to the mechanism of n425 (Figure 5). HENV-32 binding induced conformational changes in HeV G's antigenic site. Despite CedV and GhV sharing Ephrin B2 as their receptor with HeV and NiV (Table 1), neither antibody cross-reacted with them. Both HENV-26 and HENV-32 protected ferrets from lethal virus challenge, while control groups showed typical henipavirus infection symptoms. Viral RNA was detected in HENV-26 treated ferrets but not in the HENV-32 group.

2.5. HENV-103 and HENV-117 (Human)

In the following study, 41 distinct HeV/NiV G-specific antibodies were isolated from the same subject [67]. Epitope competition assays defined six major antigenic sites (A-F). Groups A and C exhibited cross-reactivity and cross-neutralization against HeV, NiV-M, and NiV-B. Group A (m102.4 included) mAb HENV-98 recognized a region overlapping with the receptor binding site. HENV-117 from Group A displayed the highest neutralizing potency among published henipavirus antibodies. Group D antibodies also neutralized three viral strains but approximately 10 times less effectively than Group A. HENV-107, representing Group D, likely binds at the interface between protomers within the HeV G tetramer's dimer-of-dimers structure, which is important for fusion triggering. Group C showed limited cross-neutralization of HeV and NiV. Groups B and E effectively neutralized HeV but not NiV. Group F antibodies were weakly neutralizing or non-neutralizing, targeting opposite sides of the receptor-binding region. The authors classified antibodies as "receptor blocking" (decreased binding when G was pre-occupied by Ephrin B2) or "receptor enhanced" (enhanced binding in the presence of Ephrin B2). The enhanced binding likely results from conformational changes making the antibody binding site more accessible after receptor binding.

In Syrian golden hamsters challenged with NiV-B, HENV-103 and HENV-117, which recognize distinct binding sites, strong protection efficacy was demonstrated (Table 2). HENV-117 significantly enhanced HENV-103 binding to G protein by approximately 15-fold, as HENV-117 induced conformational changes similar to

Ephrin B2 binding, better exposing HENV-103's target region. This cooperative binding showed functional synergy in various virus assays. For *in vivo* protection, three antibody combination approaches were tested: antibody cocktail, dual variable domain, and Bis4Ab. Only the antibody cocktail provided complete protection against lethal NiV-B challenge. The inability of engineered antibodies to simultaneously engage two antigen-binding fragments and their shorter half-life may explain their lower potency. HENV-103 and HENV-117 offer opportunities for an antibody cocktail with protective properties against mutation escape and spillover variant viruses.

2.6. 1E5 (Monkey)

Beyond human-derived mAbs, antibodies isolated from immunized animals have been instrumental in identifying cross-reactive epitopes and advancing therapeutic candidates for henipaviruses. Eight neutralizing antibodies were isolated from rAd5-NiV-B immunized rhesus macaques [69,77]. All eight antibodies bound to NiV-B G, seven bound to NiV-M G, and only five cross-reacted with HeV G. Competition binding assays classified these antibodies into three groups: A (1A9, 1F9), B (1B6, 2E7), and C (2A4, 1D11, 1E5, 2B8). All epitopes were located in the G head domain, as antibodies reacted to both the full ectodomain and the head domain of G protein. Neutralization abilities aligned with binding data, except 1D11 failed to neutralize HeV in rHIV-henipavirus assays. The four broadly neutralizing antibodies cross-neutralized HeV G D582N, NiV-M G V507I, and HeV-g2 strains. Antibodies from all groups inhibited syncytium formation, suggesting they prevent viral invasion before membrane fusion. Most Group C antibodies significantly blocked NiV G binding to receptors; Group B showed partial blockage, while Group A failed to block receptor binding. Only 1E5 and 2A4 blocked HeV G-receptor interactions. 1E5 provided complete protection in both pre- and post-exposure hamster models at doses of 10 mg/kg and 4.5 mg/kg, respectively (Table 2). Crystal structure analysis of 1E5 with NiV-B G head domain revealed its binding at the central cavity (Figure 5B). The 1E5 epitope shows high conservation and shares greater overlapping coverage with the receptor binding site compared to m102.3.

2.7. hAH1.3 (Murine)

The murine mAb hAH1.3, developed against HeV G protein, effectively neutralizes HeV but lacks cross-neutralization activity against NiV [78]. Under selective pressure from hAH1.3, a neutralization escape mutant (S134F) in the HeV G protein emerged, substantially reducing the antibody's efficacy. Nevertheless, recent studies indicate that hAH1.3 retains neutralizing potency against the HeV genotype 2 (HeV-g2) variant, with comparable efficacy to that observed against wild-type HeV [79]. Structural analysis of the HeV G head domain in complex with hAH1.3 reveals an epitope located opposite the HENV-32 binding site and distal from the ephrin-B2 receptor binding interface (Figure 5A). As a result, hAH1.3 neither inhibits receptor binding nor induces notable conformational changes in the HeV G protein.

2.8. nAH1.3 (Murine)

mAb nAH1.3 cross-neutralizes HeV, NiV-B, and NiV-M [78], demonstrating potent neutralization against NiV-B and HeV with IC50 of 33 and 32 ng/mL, respectively, in replication-competent CedV chimeras [79]. Cryo-EM structures reveal nAH1.3 binding to each head domain of the NiV G ectodomain homotetramer (Figure 5B,C). Since nAH1.3's epitope is opposite to the receptor binding site, it doesn't compete with receptor binding to NiV G protein. As nAH1.3 doesn't alter NiV G's overall conformation or bind to the receptor binding site, its neutralizing mechanism likely involves disrupting G-F protein interaction and preventing F fusion triggering, as shown in membrane fusion assays [80]. The structure confirms previously identified neutralization-escape mutants Q450K and R516K [78], as these residues interact with nAH1.3's heavy chain. Additional escape mutants: I520T of NiV G and T117A and N186D of HeV G were identified. Importantly, m102.4 and nAH1.3 target distinct regions of the G protein, and their combined use synergistically neutralizes both HeV and NiV in rCedV chimeras.

2.9. Nip GIP 1.7, Nip 3B10 (Murine)

The mAbs Nip GIP 1.7 and Nip 3B10 were developed by immunizing BALB/c mice with plasmid DNA encoding the NiV G glycoprotein, followed by boosts with vaccinia virus recombinants expressing the same protein [71]. NiV-specific antibodies were selected using ELISA and confirmed by FACScan analysis. Both mAbs specifically target the NiV G glycoprotein and exhibit strong neutralizing activity against NiV *in vitro*, though they do not cross-neutralize HeV. *In vitro* neutralization testing showed that Nip GIP 1.7 had the highest neutralizing activity, requiring only 0.27 ng to completely neutralize 25 PFU of NiV. Nip 3B10 required 0.9 ng for the same level of neutralization. *In vivo* studies demonstrated their high potency: Nip GIP 1.7, administered at

112 μg, provided complete protection against lethal NiV challenge when given prophylactically, while even lower doses (1.12 μg) remained highly effective. Nip 3B10 showed similar protective efficacy at 100 μg (Table 2). High doses of these anti-G mAbs induced sterilizing immunity, preventing detectable viral replication, lower antibody levels protected against lethal infection but allowed viral replication, as evidenced by rising anti-NiV antibody titers beginning 18 days post-challenge. Additionally, their therapeutic window was limited, as post-infection administration protected only 50–75% of animals when given within 24 h, unlike anti-F mAbs used in the same study, which retained efficacy for up to 96 h. These findings highlight the potential of anti-G mAbs like Nip GIP 1.7 for pre-exposure prophylaxis against NiV.

2.10. Anti-G Antibody Panel

A self-assembling nanoparticle vaccine displaying the NiV G head domain induced broadly neutralizing antibody responses and completely protected hamsters against lethal NiV infection [81]. 27 NiV G specific neutralizing antibodies were isolated from immunized mice that recognized four distinct antigenic sites on the NiV G head domain, including two novel epitopes different from previously identified ones. Many of these antibodies showed high neutralizing potency against NiV pseudoviruses. Through competition ELISA, the researchers confirmed that antisera from mice immunized with the NiV G immunogen targeted these four distinct epitopes on the NiV G head domain, demonstrating the diversity of polyclonal antibody responses induced by the antigen.

3. Anti-F Neutralizing Antibodies

3.1. Antibodies Targeting Apical Epitope

Two anti-F rabbit neutralizing antibodies (mAb66 and mAb92) were isolated using DNA immunization in rabbits with codon-optimized NiV F from the Malaysia strain [82]. Both antibodies targeted conformational epitopes, with mAb66 binding equally to NiV F and HeV F while mAb92 showed stronger binding to NiV F than HeV F. mAb66 and mAb92 neutralized wild-type NiV F/G mediated viral entry with an IC50 below 1 μg/mL [82]. Later structural analysis revealed that Fab66 binds to an epitope near the apex of NiV F, specifically to domain III (DIII)—a region critical for fusion that undergoes refolding during F protein conformational changes (Figure 6) [83]. The glycosylation near mAb66's epitope doesn't impede binding. Other antibodies (HeV F specific mAb36 and polyclonal sera pAB835) target similar regions, indicating this is an immunodominant epitope inducing broadly neutralizing antibodies. mAb92 recognizes an overlapping but distinct epitope and poorly neutralizes HeV due to Asn67 glycan shielding and sequence differences [73]. Removing the Asn67 glycan significantly enhanced mAb92's binding and neutralization of HeV F. In Syrian hamster models, mAb 92 provided complete protection against lethal NiV-M challenge without clinical signs but failed to protect against HeV, consistent with its *in vitro* activity. Another murine antibody, 12B2, cross-reacting with both NiV F and HeV F, binds a novel apical epitope on the F trimer. Viral passaging under antibody pressure yielded an S191R escape mutant for 12B2. Humanized variant of 12B2 maintained neutralizing activity [84]. Additionally, 2D3 and 4H3 (murine antibodies from a separate study), also recognized apical DIII epitopes [85].

Eight rhesus-derived mAbs (6E4, 5D4, 5D5, 1G8, 5H1, 6H7, 1D6, and 3E2) competed with the apex-targeting mAb 4H3, confirming their binding to the F-trimer apex [75]. Among these, 1D6 recognized a slightly lower epitope, reducing interference from the Asn67-linked glycan. Notably, 1D6 exhibited synergistic neutralization with G-specific mAbs (1E5 and 1B6) and nearly abolished cell fusion by locking the F protein in its prefusion conformation. A single critical residue, R244, was identified as essential for 1D6 binding. In hamster models of henipavirus infection, both 1D6 and 5H1 provided complete prophylactic protection. Therapeutically, 1D6 achieved an 83.3% survival rate, outperforming 5H1 (66.7%). The long CDRH3 loops of 1D6 and 5C8 inserted into the hollows between adjacent protomers of the F-trimer. This hollow-filling interaction reinforces the F-trimer's rigidity, stabilizing the prefusion conformation and reducing sensitivity to viral variations. Most cross-neutralizing antibodies employ an IGHV4-59-like VH framework to form a pushpin-shaped paratope, enabling effective targeting.

Nanobody DS90, isolated from a bacterial display library, binds a conserved, glycan-free quaternary epitope on the lateral face of the NiV F trimer (Figure 6), a site shared across NiV-M and HeV F proteins [76]. To counter the high mutation rate of henipaviruses, a bispecific antibody (DS90-m102.4) was developed, combining anti-F (DS90) and anti-G (m102.4) targeting to minimize viral escape. This bispecific construct demonstrated enhanced neutralization against NiV-M, NiV-B, and HeV compared to its monospecific counterparts, while also exhibiting antibody-dependent cellular cytotoxicity (ADCC) activity for additional antiviral effects. In Syrian golden hamsters, a single prophylactic dose of the bispecific antibody DS90-m102.4 (10 mg/kg) provided 100% survival, demonstrating superior efficacy over monovalent antibodies. Monovalent m102.4 or 5B3 achieved only 83%

survival, while the DS90 monomer offered no protection. Even in post-exposure treatment, both DS90 Fc dimer DS90-m102.4 achieved 50% survival and delayed mortality by four days, whereas 5B3 and m102.4 showed only ~17% survival. The failure of monomeric DS90 to protect underscores the necessity of bivalent binding for efficacy. These findings position DS90-m102.4 as a promising bispecific therapeutic, leveraging dual F/G targeting to enhance protection and reduce escape mutants, warranting further development for NiV countermeasures.

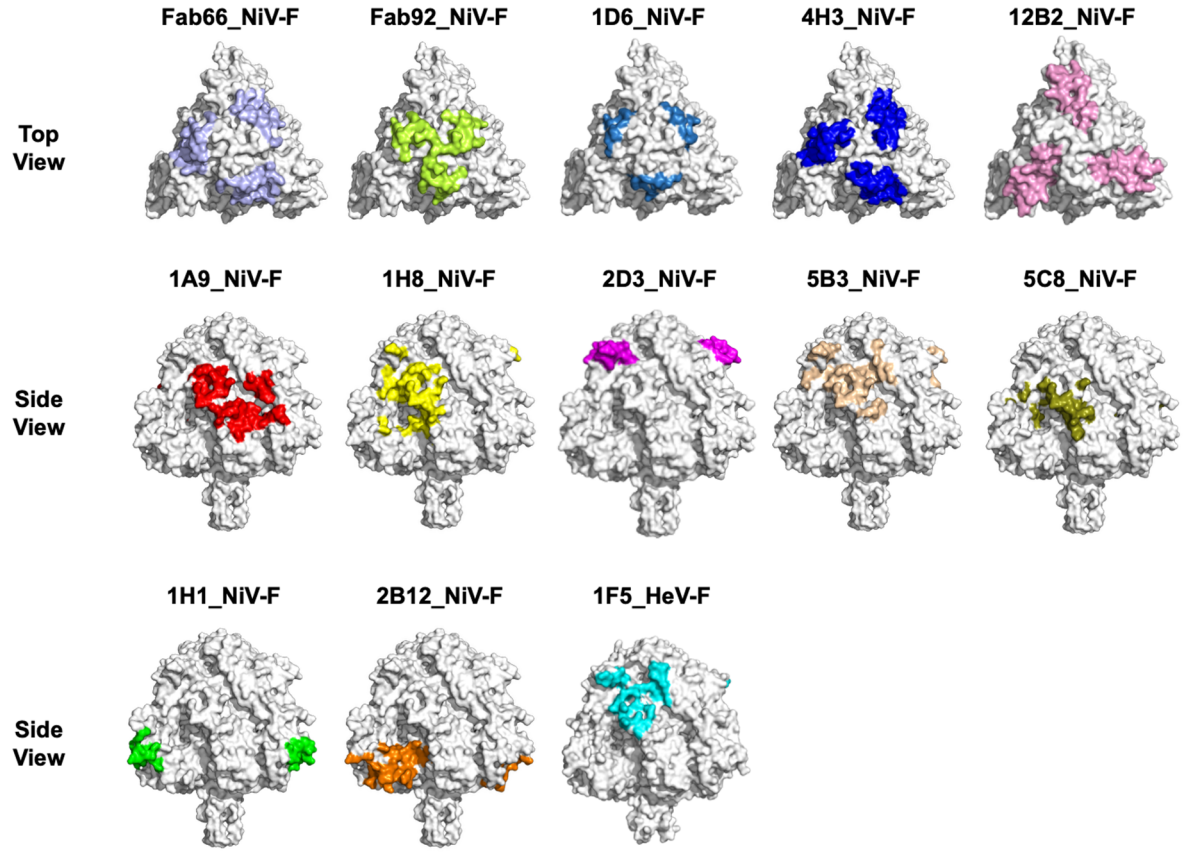

Figure 6. Epitope mapping of neutralizing antibodies against henipavirus F glycoproteins. Surface representations of the Nipah virus (NiV) F trimer in the prefusion conformation (PDB: 5EVM) are shown in top or side views depending on the epitope location, with binding sites for neutralizing antibodies highlighted: Fab66 (light blue), Fab92 (lime green), 1D6 (sky blue), 4H3 (blue), 12B2 (violet), 1A9 (red), 1H8 (yellow), 2D3 (magenta), 5B3 (peach), 5C8 (deep olive), 1H1 (green), and 2B12 (orange). The last panel shows a surface representation of the Hendra virus (HeV) F trimer (PDB: 5EJB) with the binding footprint of neutralizing antibody 1F5 (cyan). Together, these structures illustrate the diverse epitope landscape targeted by neutralizing antibodies against henipavirus F glycoproteins.

3.2. Antibodies Targeting Lateral Epitope

The murine mAb 5B3 was isolated and humanized to generate h5B3.1, which binds a specific prefusion epitope on the F glycoprotein [86,87]. Despite weaker binding affinity than its parent, h5B3.1 maintained equivalent neutralizing potency against NiV-M, NiV-B, and HeV strains. Cryo-EM structure revealed that 5B3 recognizes a quaternary epitope on DIII of the NiV F globular head (Figure 6). Passaging authentic NiV with 5B3 identified the K55E escape mutation that eliminated 5B3 binding and neutralization. Cell-cell fusion assays demonstrated that 5B3/h5B3.1 effectively inhibited F-induced fusion in a concentration-dependent manner by stabilizing F in its prefusion state, increasing the activation energy needed for fusion. Ferrets treated with h5B3.1 post-exposure to NiV and HeV survived without significant clinical symptoms or pathological signs, while control animals died (Table 2) [72]. No infectious virus was isolated from h5B3.1-treated ferrets, indicating effective viral clearance. Additionally, treated ferrets developed increased neutralizing antibody titers and seroconversion, suggesting host immune response contribution to protection.

Murine mAb 1F5 cross-reacted with NiV F and HeV F and inhibited cell-cell fusion in a concentration-dependent manner and 1F5 targets a lateral site overlapping with the 5B3 epitope (Figure 6) [85]. Competition assays indicated that 5B3 and 12B2 bind simultaneously, whereas 1F5 and 12B2 compete due to steric hindrance. Despite distinct epitopes, neither 1F5 + 12B2 nor 5B3 + 12B2 combinations showed synergistic neutralization or

fusion inhibition. In post-exposure hamster models, hu1F5, hu12B2, and a two-antibody cocktail achieved survival rates of 100%, 60%, and 80%, respectively, with hu1F5 outperforming both hu12B2 and the cocktail [74]. Subsequent AGM studies used intranasal viral delivery via a mucosal atomization device to mimic natural human exposure. At 25 mg/kg, hu1F5 conferred complete protection against lethal NiV-B challenge, while m102.4 saved only one of six animals. Even at 10 mg/kg, hu1F5 maintained robust efficacy. Although m102.4 showed higher *in vitro* neutralization potency, hu1F5's superior *in vivo* protection likely stems from its high-affinity stabilization of prefusion F, directly inhibiting fusion—a critical step under stringent infection conditions. To enhance clinical potential, an Fc-engineered variant, MBP1F5, was developed. Given its exceptional AGM results and the unmet need for henipavirus therapeutics, MBP1F5 is now advancing to Phase 1 clinical trials.

3.3. Antibodies Targeting Basal and Unknown Epitope

Mice were immunized with a NiV pre-F protein [88] and ten neutralizing mAbs were obtained [85]. Among these, nine mAbs specifically bound to the prefusion conformation, while 1H1 recognized both pre and postfusion states. Competition binding assays revealed that 1F3, 2D3, and 4H3 competed with the rabbit antibody mAb66 (targeting the NiV F apex), whereas five antibodies (1F2, 1H8, 2D3, 4B8, and 4H3) competed with 5B3 (binding the lateral-apical junction). The remaining four antibodies (1A9, 1H1, 2B12, and 4F6) did not compete with either mAb66 or 5B3, suggesting novel epitope recognition. Cryo-EM studies of six antibodies (1A9, 1H1, 1H8, 2B12, 2D3, and 4H3) revealed distinct epitopes across the prefusion NiV F protein: 2D3 and 4H3 bound apical DIII epitopes, 1H8 recognized a quaternary epitope spanning DI and DIII on adjacent protomers, 1A9 targeted a lateral DI-DII interface, 1H1 bound a basal DII-DIII quaternary epitope, and 2B12 identified a membrane-proximal DII epitope adjacent to 1H1's binding site (Figure 6). Notably, seven antibodies (1A9, 1F2, 1H1, 1H8, 2B12, 2D3, and 4F6) cross-reacted with HeV F, indicating broad applicability. Multiple sequence alignments confirmed that these neutralizing epitopes, particularly those on basal surfaces, reside in highly conserved henipavirus regions.

Two anti-F murine antibodies, Nip GIP 35 and Nip GIP 3, were isolated from immunized mice infused with plasmid and vaccinia virus recombinants expressing F protein [71]. Both antibodies cross-neutralized NiV and HeV. In hamster challenge studies, when administered 24h before and 1h after a 100 LD NiV challenge, nearly all hamsters receiving standard antibody doses survived, except for two Nip GIP 3-treated hamsters (Table 2). All control hamsters without antibody treatment died. The antibodies demonstrated a 10–13-day half-life, and no anti-NiV binding antibodies were detected via ELISA, suggesting the virus was eliminated before inducing an immune response. Full protection required at least 1.8 μg of anti-F antibody in pre-exposure models. In post-exposure studies, Nip GIP35 provided complete protection when given 1h after viral challenge and still achieved 50% survival when administered 96h post-infection.

4. Discussion

The emergence of highly pathogenic henipaviruses, including HeV, NiV, which exhibit case-fatality rates up to 100%, and newly identified species such as, MojV, LayV, CHV, poses a critical global health threat due to zoonotic spillover potential and capacity for human-to-human transmission [15,19–21]. The expanding geographic range of bat reservoirs, coupled with the discovery of novel host species (e.g., shrews, rodents), increases the likelihood of endemic establishment and pandemic spread. Recent detections, such as HeV-g2 in Australia and CHV in North American shrews, underscore the unpredictable evolutionary trajectory of this viral genus. In response, there is a pressing need to develop broad-spectrum countermeasures.

Structural and functional analyses of henipavirus glycoproteins have illuminated conserved epitopes that are promising targets for broad-spectrum neutralizing antibodies. Antibodies like m102.4 and HENV-26, which block the G glycoprotein's receptor-binding site, demonstrate cross-neutralization of HeV and NiV by targeting regions shared across strains [64,66]. However, the efficacy of m102.4 was attenuated by mutants (e.g., NiV V507I, HeV D582N), underscoring the vulnerability of single-epitope approaches [64]. In contrast, antibodies such as n425 and 1F5 recognize conserved conformational epitopes on the G tetramer or prefusion F trimer, respectively. Cryo-EM studies reveal that n425 locks the G tetramer in a fusion-incompetent state [70], while 1F5 stabilizes the F protein's prefusion conformation [74,84]. These mechanisms may provide increased resilience against point mutations compared to antibodies that bind to linear or highly variable regions. However, the henipavirus family has undergone remarkable diversification since HeV's identification in 1994, expanding from two initial species to at least 20 recognized species across six continents within three decades. This rapid evolution demonstrates how modest genetic changes can dramatically alter epidemiological characteristics: although NiV-M and NiV-B share 91.8% genome identity, they differ significantly in pathogenicity, incubation period, and human-to-human transmissibility. Functional diversification within the genus is further illustrated by altered receptor usage patterns:

while HeV and NiV utilize ephrin-B2 and ephrin-B3 receptors, Cedar virus exhibits broader tropism and reduced pathogenicity, and MojV and LayV show no binding to traditional ephrin-B receptors, indicating evolution of alternative entry mechanisms. This evolutionary dynamism underscores that even antibodies targeting conserved epitopes are not completely resistant to escape and new strains, making continued surveillance of viral evolution essential for assessing long-term therapeutic breadth and efficacy.

The narrow therapeutic window of some antibodies (e.g., m102.4's loss of efficacy beyond 5 days post-infection against NiV-B) and the rapid emergence of escape mutants (e.g., HeV S134F under hAH1.3 pressure) highlight the limitations of monotherapies [63,78]. The development of bispecific antibodies and cocktails like DS90-m102.4 and combination of m102.4 + nAH1.3 or HENV-103 and HENV-117 represent a sophisticated approach to addressing viral escape and enhancing neutralization potency [76]. Simultaneously targeting both F and G glycoproteins, or different epitopes of one antigen, theoretically provide multiple mechanisms of action: receptor blocking through G-protein engagement, fusion inhibition through F-protein stabilization and enhanced epitope accessibility. This multiple targeting reduces the probability of escape mutants that would need to simultaneously develop resistance to both epitopes. However, the engineering challenges for bispecific antibodies are substantial. The manuscript reveals that engineered formats like dual variable domains and BiS4Ab constructs failed to provide the protection observed with simple antibody cocktails, likely due to constraints in simultaneous antigen engagement and reduced half-life. This suggests that optimal bispecific design requires careful attention to linker length, antibody orientation, and pharmacokinetic properties.

While animal models have been instrumental in advancing henipavirus antibody therapeutics, several inherent limitations may affect the translation of preclinical findings to human clinical outcomes [89–92]. Hamster models typically show rapid, acute disease courses that may not reflect the variable clinical presentations observed in human henipavirus infections, thereby exaggerating the apparent narrow therapeutic window of candidate antibodies [71,91]. Ferret models recapitulate multisystemic vasculitis, but may not accurately predict the neurologic manifestations that dominate severe human Nipah virus infection [58,93,94]. Differences in Fc receptor biology and immune system regulation between nonhuman primates and humans may affect the pharmacodynamics of antibody therapeutics. Moreover, the controlled timing of challenge and treatment in animal studies does not replicate the heterogeneous clinical contexts of human exposures, where patients may present late in infection. These limitations highlight the importance of cautious interpretation of animal efficacy data and underscore the need for complementary approaches to validate the true translational potential of antibody therapeutics against henipaviruses.

The rapidly evolving henipavirus landscape calls for a shift from strain-specific interventions toward broad-spectrum, structure-guided immunotherapeutics. By leveraging conserved viral epitopes, multi-epitope antibody strategies, and optimized delivery technologies, the field can advance toward preemptive solutions capable of containing future outbreaks. As climate change and ecological disruption continue to intensify human-wildlife interactions, such approaches will be vital for interrupting zoonotic transmission and safeguarding global health.

Author Contributions: J.H. and K.X.: conceptualization; J.H.: draft preparation; Y.Z., E.H.Z., E.K., Z.S. and K.X.: reviewing and editing. All authors have read and agreed to the published version of the manuscript.

Funding: This research received no external funding.

Institutional Review Board Statement: Not applicable.

Informed Consent Statement: Not applicable.

Data Availability Statement: Not applicable.

Conflicts of Interest: The authors declare no conflict of interest.

Use of AI and AI-Assisted Technologies: During manuscript preparation, DeepSeek was used solely to enhance language clarity and readability. The authors subsequently reviewed and edited the content and assume full responsibility for the publication.

References

1. Eaton, B.T.; Broder, C.C.; Middleton, D.; Wang, L.-F. Hendra and Nipah viruses: Different and dangerous. *Nat. Rev. Microbiol.* **2006**, *4*, 23–35. https://doi.org/10.1038/nrmicro1323.
2. Quarleri, J.; Galvan, V.; Delpino, M.V. Henipaviruses: An expanding global public health concern? *GeroScience* **2022**, *44*, 2447–2459. https://doi.org/10.1007/s11357-022-00670-9.
3. Wang, L.F.; Yu, M.; Hansson, E.; Pritchard, L.I.; Shiell, B.; Michalski, W.P.; Eaton, B.T. The exceptionally large genome of Hendra virus: Support for creation of a new genus within the family Paramyxoviridae. *J. Virol.* **2000**, *74*, 9972–9979. https://doi.org/10.1128/jvi.74.21.9972-9979.2000.

4. Harcourt, B.H.; Tamin, A.; Halpin, K.; Ksiazek, T.G.; Rollin, P.E.; Bellini, W.J.; Rota, P.A. Molecular characterization of the polymerase gene and genomic termini of Nipah virus. *Virology* **2001**, *287*, 192–201. https://doi.org/10.1006/viro.2001.1026.
5. Ker, D.-S.; Jenkins, H.T.; Greive, S.J.; Antson, A.A. CryoEM structure of the Nipah virus nucleocapsid assembly. *PLoS Pathog.* **2021**, *17*, e1009740. https://doi.org/10.1371/journal.ppat.1009740.
6. Species List: *Paramyxoviridae*. Available online: https://ictv.global/report/chapter/paramyxoviridae/taxonomy/paramyxoviridae (accessed on 1 December 2026)
7. Murray, K.; Rogers, R.; Selvey, L.; Selleck, P.; Hyatt, A.; Gould, A.; Gleeson, L.; Hooper, P.; Westbury, H. A novel morbillivirus pneumonia of horses and its transmission to humans. *Emerg. Infect. Dis.* **1995**, *1*, 31–33. https://doi.org/10.3201/eid0101.950107.
8. Murray, K.; Selleck, P.; Hooper, P.; Hyatt, A.; Gould, A.; Gleeson, L.; Westbury, H.; Hiley, L.; Selvey, L.; Rodwell, B. A morbillivirus that caused fatal disease in horses and humans. *Science* **1995**, *268*, 94–97. https://doi.org/10.1126/science.7701348.
9. Paton, N.I.; Leo, Y.S.; Zaki, S.R.; Auchus, A.P.; Lee, K.E.; Ling, A.E.; Chew, S.K.; Ang, B.; Rollin, P.E.; Umapathi, T.; et al. Outbreak of Nipah-virus infection among abattoir workers in Singapore. *Lancet* **1999**, *354*, 1253–1256. https://doi.org/10.1016/S0140-6736(99)04379-2.
10. Chua, K.B.; Bellini, W.J.; Rota, P.A.; Harcourt, B.H.; Tamin, A.; Lam, S.K.; Ksiazek, T.G.; Rollin, P.E.; Zaki, S.R.; Shieh, W.; et al. Nipah virus: A recently emergent deadly paramyxovirus. *Science* **2000**, *288*, 1432–1435. https://doi.org/10.1126/science.288.5470.1432.
11. Chua, K.B. Nipah virus outbreak in Malaysia. *J. Clin. Virol.* **2003**, *26*, 265–275. https://doi.org/10.1016/s1386-6532(02)00268-8.
12. Khan, S.; Akbar, S.M.F.; Mahtab, M.A.; Uddin, M.N.; Rashid, M.M.; Yahiro, T.; Hashimoto, T.; Kimitsuki, K.; Nishizono, A. Twenty-five years of Nipah outbreaks in Southeast Asia: A persistent threat to global health. *IJID Reg.* **2024**, *13*, 100434. https://doi.org/10.1016/j.ijregi.2024.100434.
13. Drexler, J.F.; Corman, V.M.; Müller, M.A.; Maganga, G.D.; Vallo, P.; Binger, T.; Gloza-Rausch, F.; Cottontail, V.M.; Rasche, A.; Yordanov, S.; et al. Bats host major mammalian paramyxoviruses. *Nat. Commun.* **2012**, *3*, 796. https://doi.org/10.1038/ncomms1796.
14. Marsh, G.A.; de Jong, C.; Barr, J.A.; Tachedjian, M.; Smith, C.; Middleton, D.; Yu, M.; Todd, S.; Foord, A.J.; Haring, V.; et al. Cedar virus: A novel Henipavirus isolated from Australian bats. *PLoS Pathog.* **2012**, *8*, e1002836. https://doi.org/10.1371/journal.ppat.1002836.
15. Wu, Z.; Yang, L.; Yang, F.; Ren, X.; Jiang, J.; Dong, J.; Sun, L.; Zhu, Y.; Zhou, H.; Jin, Q. Novel Henipa-like virus, Mojiang Paramyxovirus, in rats, China, 2012. *Emerg. Infect. Dis.* **2014**, *20*, 1064–1066. https://doi.org/10.3201/eid2006.131022.
16. Kuang, G.; Yang, T.; Yang, W.; Wang, J.; Pan, H.; Pan, Y.; Gou, Q.Y.; Wu, W.C.; Wang, J.; Yang, L.; et al. Infectome analysis of bat kidneys from Yunnan province, China, reveals novel henipaviruses related to Hendra and Nipah viruses and prevalent bacterial and eukaryotic microbes. *PLoS Pathog.* **2025**, *21*, e1013235. https://doi.org/10.1371/journal.ppat.1013235.
17. Lee, S.H.; Kim, K.; Kim, J.; No, J.S.; Park, K.; Budhathoki, S.; Lee, S.H.; Lee, J.; Cho, S.H.; Cho, S.; et al. Discovery and Genetic Characterization of Novel Paramyxoviruses Related to the Genus *Henipavirus* in Crocidura Species in the Republic of Korea. *Viruses* **2021**, *13*, 2020. https://doi.org/10.3390/v13102020.
18. Kaza, B.; Aguilar, H.C. Pathogenicity and virulence of henipaviruses. *Virulence* **2023**, *14*, 2273684. https://doi.org/10.1080/21505594.2023.2273684.
19. Taylor, J.; Thompson, K.; Annand, E.J.; Massey, P.D.; Bennett, J.; Eden, J.-S.; Horsburgh, B.A.; Hodgson, E.; Wood, K.; Kerr, J.; et al. Novel variant Hendra virus genotype 2 infection in a horse in the greater Newcastle region, New South Wales, Australia. *One Health* **2022**, *15*, 100423. https://doi.org/10.1016/j.onehlt.2022.100423.
20. Parry, R.H.; Yamada, K.Y.H.; Hood, W.R.; Zhao, Y.; Lu, J.Y.; Seluanov, A.; Gorbunova, V.; Modhiran, N.; Watterson, D.; Isaacs, A. Henipavirus in northern short-tailed shrew, Alabama, USA. *Emerg. Infect. Dis.* **2025**, *31*, 392–394. https://doi.org/10.3201/eid3102.241155.
21. Zhang, X.A.; Li, H.; Jiang, F.C.; Zhu, F.; Zhang, Y.F.; Chen, J.J.; Tan, C.W.; Anderson, D.E.; Fan, H.; Dong, L.Y.; et al. A Zoonotic Henipavirus in Febrile Patients in China. *N. Engl. J. Med.* **2022**, *387*, 470–472. https://doi.org/10.1056/NEJMc2202705.
22. Hernández, L.H.A.; da Paz, T.Y.B.; Silva, S.P.D.; Silva, F.S.D.; Barros, B.C.V.; Nunes, B.T.D.; Casseb, L.M.N.; Medeiros, D.B.A.; Vasconcelos, P.; Cruz, A.C.R. First Genomic Evidence of a Henipa-like Virus in Brazil. *Viruses* **2022**, *14*, 2167. https://doi.org/10.3390/v14102167.
23. Vanmechelen, B.; Meurs, S.; Horemans, M.; Loosen, A.; Joly Maes, T.; Laenen, L.; Vergote, V.; Koundouno, F.R.; Magassouba, N.; Konde, M.K.; et al. The characterization of multiple novel paramyxoviruses highlights the diverse nature of the subfamily *Orthoparamyxovirinae*. *Virus Evol* **2022**, *8*, veac061. https://doi.org/10.1093/ve/veac061.

24. Madera, S.; Kistler, A.; Ranaivoson, H.C.; Ahyong, V.; Andrianiaina, A.; Andry, S.; Raharinosy, V.; Randriambolamanantsoa, T.H.; Ravelomanantsoa, N.A.F.; Tato, C.M.; et al. Discovery and Genomic Characterization of a Novel Henipavirus, Angavokely Virus, from Fruit Bats in Madagascar. *J. Virol.* **2022**, *96*, e0092122. https://doi.org/10.1128/jvi.00921-22.
25. Clayton, B.A.; Wang, L.F.; Marsh, G.A. Henipaviruses: An updated review focusing on the pteropid reservoir and features of transmission: Henipaviruses: The pteropid reservoir and features of transmission. *Zoonoses Public Health* **2013**, *60*, 69–83. https://doi.org/10.1111/j.1863-2378.2012.01501.x.
26. Epstein, J.H.; Anthony, S.J.; Islam, A.; Kilpatrick, A.M.; Ali Khan, S.; Balkey, M.D.; Ross, N.; Smith, I.; Zambrana-Torrelio, C.; Tao, Y.; et al. Nipah virus dynamics in bats and implications for spillover to humans. *Proc. Natl. Acad. Sci. USA* **2020**, *117*, 29190–29201. https://doi.org/10.1073/pnas.2000429117.
27. Garbuglia, A.R.; Lapa, D.; Pauciullo, S.; Raoul, H.; Pannetier, D. Nipah virus: An overview of the current status of diagnostics and their role in preparedness in endemic countries. *Viruses* **2023**, *15*, 2062. https://doi.org/10.3390/v15102062.
28. Rahman, M.Z.; Islam, M.M.; Hossain, M.E.; Rahman, M.M.; Islam, A.; Siddika, A.; Hossain, M.S.S.; Sultana, S.; Islam, A.; Rahman, M.; et al. Genetic diversity of Nipah virus in Bangladesh. *Int. J. Infect. Dis.* **2021**, *102*, 144–151. https://doi.org/10.1016/j.ijid.2020.10.041.
29. Halpin, K.; Rota, P.A. A Review of Hendra Virus and Nipah Virus Infections in Man and Other Animals. In *Zoonoses: Infections Affecting Humans and Animals*, Sing, A., Ed.; Springer International Publishing: Cham, Switzerland, 2023; pp. 1493–1508.
30. Singh, R.K.; Dhama, K.; Chakraborty, S.; Tiwari, R.; Natesan, S.; Khandia, R.; Munjal, A.; Vora, K.S.; Latheef, S.K.; Karthik, K.; et al. Nipah virus: Epidemiology, pathology, immunobiology and advances in diagnosis, vaccine designing and control strategies—A comprehensive review. *Vet. Q.* **2019**, *39*, 26–55. https://doi.org/10.1080/01652176.2019.1580827.
31. O'Sullivan, J.D.; Allworth, A.M.; Paterson, D.L.; Snow, T.M.; Boots, R.; Gleeson, L.J.; Gould, A.R.; Hyatt, A.D.; Bradfield, J. Fatal encephalitis due to novel paramyxovirus transmitted from horses. *Lancet* **1997**, *349*, 93–95. https://doi.org/10.1016/s0140-6736(96)06162-4.
32. Wong, K.T.; Shieh, W.-J.; Kumar, S.; Norain, K.; Abdullah, W.; Guarner, J.; Goldsmith, C.S.; Chua, K.B.; Lam, S.K.; Tan, C.T.; et al. Nipah virus infection: Pathology and pathogenesis of an emerging paramyxoviral zoonosis. *Am. J. Pathol.* **2002**, *161*, 2153–2167. https://doi.org/10.1016/S0002-9440(10)64493-8.
33. Enchéry, F.; Horvat, B. Understanding the interaction between henipaviruses and their natural host, fruit bats: Paving the way toward control of highly lethal infection in humans. *Int. Rev. Immunol.* **2017**, *36*, 108–121. https://doi.org/10.1080/08830185.2016.1255883.
34. Wang, Z.; Amaya, M.; Addetia, A.; Dang, H.V.; Reggiano, G.; Yan, L.; Hickey, A.C.; DiMaio, F.; Broder, C.C.; Veesler, D. Architecture and antigenicity of the Nipah virus attachment glycoprotein. *Science* **2022**, *375*, 1373–1378. https://doi.org/10.1126/science.abm5561.
35. Guo, Y.; Wu, S.; Li, W.; Yang, H.; Shi, T.; Ju, B.; Zhang, Z.; Yan, R. The cryo-EM structure of homotetrameric attachment glycoprotein from langya henipavirus. *Nat. Commun.* **2024**, *15*, 812. https://doi.org/10.1038/s41467-024-45202-5.
36. Laing, E.D.; Navaratnarajah, C.K.; Cheliout Da Silva, S.; Petzing, S.R.; Xu, Y.; Sterling, S.L.; Marsh, G.A.; Wang, L.F.; Amaya, M.; Nikolov, D.B.; et al. Structural and functional analyses reveal promiscuous and species specific use of ephrin receptors by Cedar virus. *Proc. Natl. Acad. Sci. USA* **2019**, *116*, 20707–20715. https://doi.org/10.1073/pnas.1911773116.
37. Pager, C.T.; Dutch, R.E. Cathepsin L is involved in proteolytic processing of the Hendra virus fusion protein. *J. Virol.* **2005**, *79*, 12714–12720. https://doi.org/10.1128/JVI.79.20.12714-12720.2005.
38. Diederich, S.; Thiel, L.; Maisner, A. Role of endocytosis and cathepsin-mediated activation in Nipah virus entry. *Virology* **2008**, *375*, 391–400. https://doi.org/10.1016/j.virol.2008.02.019.
39. Diederich, S.; Sauerhering, L.; Weis, M.; Altmeppen, H.; Schaschke, N.; Reinheckel, T.; Erbar, S.; Maisner, A. Activation of the Nipah virus fusion protein in MDCK cells is mediated by cathepsin B within the endosome-recycling compartment. *J. Virol.* **2012**, *86*, 3736–3745. https://doi.org/10.1128/JVI.06628-11.
40. Xu, K.; Chan, Y.P.; Bradel-Tretheway, B.; Akyol-Ataman, Z.; Zhu, Y.; Dutta, S.; Yan, L.; Feng, Y.; Wang, L.F.; Skiniotis, G.; et al. Crystal Structure of the Pre-fusion Nipah Virus Fusion Glycoprotein Reveals a Novel Hexamer-of-Trimers Assembly. *PLoS Pathog.* **2015**, *11*, e1005322. https://doi.org/10.1371/journal.ppat.1005322.
41. Wong, J.J.; Paterson, R.G.; Lamb, R.A.; Jardetzky, T.S. Structure and stabilization of the Hendra virus F glycoprotein in its prefusion form. *Proc. Natl. Acad. Sci. USA* **2016**, *113*, 1056–1061. https://doi.org/10.1073/pnas.1523303113.
42. Wong, J.J.W.; Young, T.A.; Zhang, J.; Liu, S.; Leser, G.P.; Komives, E.A.; Lamb, R.A.; Zhou, Z.H.; Salafsky, J.; Jardetzky, T.S. Monomeric ephrinB2 binding induces allosteric changes in Nipah virus G that precede its full activation. *Nat. Commun.* **2017**, *8*, 781. https://doi.org/10.1038/s41467-017-00863-3.
43. Liu, Q.; Stone, J.A.; Bradel-Tretheway, B.; Dabundo, J.; Benavides Montano, J.A.; Santos-Montanez, J.; Biering, S.B.; Nicola, A.V.; Iorio, R.M.; Lu, X.; et al. Unraveling a three-step spatiotemporal mechanism of triggering of receptor-induced Nipah virus fusion and cell entry. *PLoS Pathog.* **2013**, *9*, e1003770. https://doi.org/10.1371/journal.ppat.1003770.

44. Liu, Q.; Bradel-Tretheway, B.; Monreal, A.I.; Saludes, J.P.; Lu, X.; Nicola, A.V.; Aguilar, H.C. Nipah virus attachment glycoprotein stalk C-terminal region links receptor binding to fusion triggering. *J. Virol.* **2015**, *89*, 1838–1850. https://doi.org/10.1128/jvi.02277-14.
45. Lizbeth Reyes Zamora, J.; Ortega, V.; Johnston, G.P.; Li, J.; André, N.M.; Abrrey Monreal, I.; Contreras, E.M.; Whittaker, G.R.; Aguilar, H.C. Third Helical Domain of the Nipah Virus Fusion Glycoprotein Modulates both Early and Late Steps in the Membrane Fusion Cascade. *J. Virol.* **2020**, *94*. https://doi.org/10.1128/jvi.00644-20.
46. Negrete, O.A.; Wolf, M.C.; Aguilar, H.C.; Enterlein, S.; Wang, W.; Mühlberger, E.; Su, S.V.; Bertolotti-Ciarlet, A.; Flick, R.; Lee, B. Two key residues in ephrinB3 are critical for its use as an alternative receptor for Nipah virus. *PLoS Pathog.* **2006**, *2*, e7. https://doi.org/10.1371/journal.ppat.0020007.
47. Xu, K.; Chan, Y.P.; Rajashankar, K.R.; Khetawat, D.; Yan, L.; Kolev, M.V.; Broder, C.C.; Nikolov, D.B. New insights into the Hendra virus attachment and entry process from structures of the virus G glycoprotein and its complex with Ephrin-B2. *PLoS ONE* **2012**, *7*, e48742. https://doi.org/10.1371/journal.pone.0048742.
48. Lee, B.; Pernet, O.; Ahmed, A.A.; Zeltina, A.; Beaty, S.M.; Bowden, T.A. Molecular recognition of human ephrinB2 cell surface receptor by an emergent African henipavirus. *Proc. Natl. Acad. Sci. USA* **2015**, *112*, E2156–E2165. https://doi.org/10.1073/pnas.1501690112.
49. Li, Y.; Li, R.; Wang, M.; Liu, Y.; Yin, Y.; Zai, X.; Song, X.; Chen, Y.; Xu, J.; Chen, W. Fc-Based Recombinant Henipavirus Vaccines Elicit Broad Neutralizing Antibody Responses in Mice. *Viruses* **2020**, *12*, 480. https://doi.org/10.3390/v12040480.
50. Wang, C.; Li, M.; Wang, Y.; Ding, Q.; Fan, S.; Lan, J. Structural insights into the Langya virus attachment glycoprotein. *Structure* **2024**, *32*, 1090–1098.e1093. https://doi.org/10.1016/j.str.2024.05.003.
51. Broder, C.C.; Xu, K.; Nikolov, D.B.; Zhu, Z.; Dimitrov, D.S.; Middleton, D.; Pallister, J.; Geisbert, T.W.; Bossart, K.N.; Wang, L.-F. A treatment for and vaccine against the deadly Hendra and Nipah viruses. *Antivir. Res.* **2013**, *100*, 8–13. https://doi.org/10.1016/j.antiviral.2013.06.012.
52. Geisbert, T.W.; Bobb, K.; Borisevich, V.; Geisbert, J.B.; Agans, K.N.; Cross, R.W.; Prasad, A.N.; Fenton, K.A.; Yu, H.; Fouts, T.R.; et al. A single dose investigational subunit vaccine for human use against Nipah virus and Hendra virus. *NPJ Vaccines* **2021**, *6*, 23. https://doi.org/10.1038/s41541-021-00284-w.
53. Halpin, K.; Graham, K.; Durr, P.A. Sero-monitoring of horses demonstrates the equivac® HeV Hendra virus vaccine to be highly effective in inducing neutralising antibody titres. *Vaccines* **2021**, *9*, 731. https://doi.org/10.3390/vaccines9070731.
54. Playford, E.G.; Munro, T.; Mahler, S.M.; Elliott, S.; Gerometta, M.; Hoger, K.L.; Jones, M.L.; Griffin, P.; Lynch, K.D.; Carroll, H.; et al. Safety, tolerability, pharmacokinetics, and immunogenicity of a human monoclonal antibody targeting the G glycoprotein of henipaviruses in healthy adults: A first-in-human, randomised, controlled, phase 1 study. *Lancet Infect. Dis.* **2020**, *20*, 445–454. https://doi.org/10.1016/S1473-3099(19)30634-6.
55. Steffen, D.L.; Xu, K.; Nikolov, D.B.; Broder, C.C. Henipavirus mediated membrane fusion, virus entry and targeted therapeutics. *Viruses* **2012**, *4*, 280–308. https://doi.org/10.3390/v4020280.
56. Zhu, Z.; Dimitrov, A.S.; Bossart, K.N.; Crameri, G.; Bishop, K.A.; Choudhry, V.; Mungall, B.A.; Feng, Y.-R.; Choudhary, A.; Zhang, M.-Y.; et al. Potent neutralization of Hendra and Nipah viruses by human monoclonal antibodies. *J. Virol.* **2006**, *80*, 891–899. https://doi.org/10.1128/JVI.80.2.891-899.2006.
57. Zhu, Z.; Bossart, K.N.; Bishop, K.A.; Crameri, G.; Dimitrov, A.S.; McEachern, J.A.; Feng, Y.; Middleton, D.; Wang, L.F.; Broder, C.C.; et al. Exceptionally potent cross-reactive neutralization of Nipah and Hendra viruses by a human monoclonal antibody. *J. Infect. Dis.* **2008**, *197*, 846–853. https://doi.org/10.1086/528801.
58. Bossart, K.N.; Zhu, Z.; Middleton, D.; Klippel, J.; Crameri, G.; Bingham, J.; McEachern, J.A.; Green, D.; Hancock, T.J.; Chan, Y.-P.; et al. A neutralizing human monoclonal antibody protects against lethal disease in a new ferret model of acute nipah virus infection. *PLoS Pathog.* **2009**, *5*, e1000642. https://doi.org/10.1371/journal.ppat.1000642.
59. Geisbert, T.W.; Daddario-DiCaprio, K.M.; Hickey, A.C.; Smith, M.A.; Chan, Y.-P.; Wang, L.-F.; Mattapallil, J.J.; Geisbert, J.B.; Bossart, K.N.; Broder, C.C. Development of an acute and highly pathogenic nonhuman primate model of Nipah virus infection. *PLoS ONE* **2010**, *5*, e10690. https://doi.org/10.1371/journal.pone.0010690.
60. Rockx, B.; Bossart, K.N.; Feldmann, F.; Geisbert, J.B.; Hickey, A.C.; Brining, D.; Callison, J.; Safronetz, D.; Marzi, A.; Kercher, L.; et al. A novel model of lethal Hendra virus infection in African green monkeys and the effectiveness of ribavirin treatment. *J. Virol.* **2010**, *84*, 9831–9839. https://doi.org/10.1128/JVI.01163-10.
61. Bossart, K.N.; Geisbert, T.W.; Feldmann, H.; Zhu, Z.; Feldmann, F.; Geisbert, J.B.; Yan, L.; Feng, Y.R.; Brining, D.; Scott, D.; et al. A neutralizing human monoclonal antibody protects african green monkeys from hendra virus challenge. *Sci. Transl. Med.* **2011**, *3*, 105ra103. https://doi.org/10.1126/scitranslmed.3002901.
62. Geisbert, T.W.; Mire, C.E.; Geisbert, J.B.; Chan, Y.P.; Agans, K.N.; Feldmann, F.; Fenton, K.A.; Zhu, Z.; Dimitrov, D.S.; Scott, D.P.; et al. Therapeutic treatment of Nipah virus infection in nonhuman primates with a neutralizing human monoclonal antibody. *Sci. Transl. Med.* **2014**, *6*, 242ra282. https://doi.org/10.1126/scitranslmed.3008929.

63. Mire, C.E.; Satterfield, B.A.; Geisbert, J.B.; Agans, K.N.; Borisevich, V.; Yan, L.; Chan, Y.-P.; Cross, R.W.; Fenton, K.A.; Broder, C.C.; et al. Pathogenic differences between nipah virus Bangladesh and Malaysia strains in primates: Implications for antibody therapy. *Sci. Rep.* **2016**, *6*, 30916. https://doi.org/10.1038/srep30916.
64. Xu, K.; Rockx, B.; Xie, Y.; DeBuysscher, B.L.; Fusco, D.L.; Zhu, Z.; Chan, Y.P.; Xu, Y.; Luu, T.; Cer, R.Z.; et al. Crystal structure of the Hendra virus attachment G glycoprotein bound to a potent cross-reactive neutralizing human monoclonal antibody. *PLoS Pathog.* **2013**, *9*, e1003684. https://doi.org/10.1371/journal.ppat.1003684.
65. Bowden, T.A.; Aricescu, A.R.; Gilbert, R.J.C.; Grimes, J.M.; Jones, E.Y.; Stuart, D.I. Structural basis of Nipah and Hendra virus attachment to their cell-surface receptor ephrin-B2. *Nat. Struct. Mol. Biol.* **2008**, *15*, 567–572. https://doi.org/10.1038/nsmb.1435.
66. Dong, J.; Cross, R.W.; Doyle, M.P.; Kose, N.; Mousa, J.J.; Annand, E.J.; Borisevich, V.; Agans, K.N.; Sutton, R.; Nargi, R.; et al. Potent Henipavirus Neutralization by Antibodies Recognizing Diverse Sites on Hendra and Nipah Virus Receptor Binding Protein. *Cell* **2020**, *183*, 1536–1550 e1517. https://doi.org/10.1016/j.cell.2020.11.023.
67. Doyle, M.P.; Kose, N.; Borisevich, V.; Binshtein, E.; Amaya, M.; Nagel, M.; Annand, E.J.; Armstrong, E.; Bombardi, R.; Dong, J.; et al. Cooperativity mediated by rationally selected combinations of human monoclonal antibodies targeting the henipavirus receptor binding protein. *Cell Rep.* **2021**, *36*, 109628. https://doi.org/10.1016/j.celrep.2021.109628.
68. Chen, L.; Sun, M.; Zhang, H.; Zhang, X.; Yao, Y.; Li, M.; Li, K.; Fan, P.; Zhang, H.; Qin, Y.; et al. Potent human neutralizing antibodies against Nipah virus derived from two ancestral antibody heavy chains. *Nat. Commun.* **2024**, *15*, 2987. https://doi.org/10.1038/s41467-024-47213-8.
69. Fan, P.; Sun, M.; Zhang, X.; Zhang, H.; Liu, Y.; Yao, Y.; Li, M.; Fang, T.; Sun, B.; Chen, Z.; et al. A potent Henipavirus cross-neutralizing antibody reveals a dynamic fusion-triggering pattern of the G-tetramer. *Nat. Commun.* **2024**, *15*, 4330. https://doi.org/10.1038/s41467-024-48601-w.
70. Wang, Y.; Sun, Y.; Shen, Z.; Wang, C.; Qian, J.; Mao, Q.; Wang, Y.; Song, W.; Kong, Y.; Zhan, C.; et al. Fully human single-domain antibody targeting a highly conserved cryptic epitope on the Nipah virus G protein. *Nat. Commun.* **2024**, *15*, 6892. https://doi.org/10.1038/s41467-024-51066-6.
71. Guillaume, V.; Contamin, H.; Loth, P.; Grosjean, I.; Courbot, M.C.G.; Deubel, V.; Buckland, R.; Wild, T.F. Antibody prophylaxis and therapy against Nipah virus infection in hamsters. *J. Virol.* **2006**, *80*, 1972–1978. https://doi.org/10.1128/JVI.80.4.1972-1978.2006.
72. Mire, C.E.; Chan, Y.-P.; Borisevich, V.; Cross, R.W.; Yan, L.; Agans, K.N.; Dang, H.V.; Veesler, D.; Fenton, K.A.; Geisbert, T.W.; et al. A cross-reactive humanized monoclonal antibody targeting fusion glycoprotein function protects ferrets against lethal nipah virus and Hendra virus infection. *J. Infect. Dis.* **2020**, *221*, S471–S479. https://doi.org/10.1093/infdis/jiz515.
73. Avanzato, V.A.; Bushmaker, T.; Oguntuyo, K.Y.; Yinda, C.K.; Duyvesteyn, H.M.E.; Stass, R.; Meade-White, K.; Rosenke, R.; Thomas, T.; van Doremalen, N.; et al. A monoclonal antibody targeting the Nipah virus fusion glycoprotein apex imparts protection from disease. *J. Virol.* **2024**, *98*, e0063824. https://doi.org/10.1128/jvi.00638-24.
74. Zeitlin, L.; Cross, R.W.; Woolsey, C.; West, B.R.; Borisevich, V.; Agans, K.N.; Prasad, A.N.; Deer, D.J.; Stuart, L.; McCavitt-Malvido, M.; et al. Therapeutic administration of a cross-reactive mAb targeting the fusion glycoprotein of Nipah virus protects nonhuman primates. *Sci. Transl. Med.* **2024**, *16*, eadl2055. https://doi.org/10.1126/scitranslmed.adl2055.
75. Ren, Y.; Fan, P.; Zhang, X.; Fang, T.; Chen, Z.; Yao, Y.; Chi, X.; Zhang, G.; Zhao, X.; Sun, B.; et al. Potent Cross-neutralizing Antibodies Reveal Vulnerabilities of Henipavirus Fusion Glycoprotein. *Adv. Sci.* **2025**, *12*, e2501996. https://doi.org/10.1002/advs.202501996.
76. Isaacs, A.; Nieto, G.V.; Zhang, X.; Modhiran, N.; Barr, J.; Thakur, N.; Low, Y.S.; Parry, R.H.; Barnes, J.B.; Jara, R.; et al. A protective bispecific antibody targets both Nipah virus surface glycoproteins and limits viral escape. *bioRxiv* **2025**. https://doi.org/10.1101/2025.03.11.642517.
77. Huang, X.; Li, Y.; Li, R.; Wang, S.; Yang, L.; Wang, S.; Yin, Y.; Zai, X.; Zhang, J.; Xu, J. Nipah virus attachment glycoprotein ectodomain delivered by type 5 adenovirus vector elicits broad immune response against NiV and HeV. *Front. Cell. Infect. Microbiol.* **2023**, *13*, 1180344. https://doi.org/10.3389/fcimb.2023.1180344.
78. Borisevich, V.; Lee, B.; Hickey, A.; DeBuysscher, B.; Broder, C.C.; Feldmann, H.; Rockx, B. Escape From Monoclonal Antibody Neutralization Affects Henipavirus Fitness *In Vitro* and *In Vivo*. *J. Infect. Dis.* **2016**, *213*, 448–455. https://doi.org/10.1093/infdis/jiv449.
79. Wang, Z.; Dang, H.V.; Amaya, M.; Xu, Y.; Yin, R.; Yan, L.; Hickey, A.C.; Annand, E.J.; Horsburgh, B.A.; Reid, P.A.; et al. Potent monoclonal antibody-mediated neutralization of a divergent Hendra virus variant. *Proc. Natl. Acad. Sci. USA* **2022**, *119*, e2122769119. https://doi.org/10.1073/pnas.2122769119.
80. Hickey, A.C. Defining the Antigenic Structure of the Henipavirus Attachment (G) Glycoprotein: Implications for the Fusion Mechanism. Ph.D. Thesis, Uniformed Services University of the Health Sciences, Bethesda,MD, USA, 2009.

81. Zhou, D.; Cheng, R.; Yao, Y.; Zhang, G.; Li, X.; Wang, B.; Wang, Y.; Yu, F.; Yang, S.; Liu, H.; et al. An attachment glycoprotein nanoparticle elicits broadly neutralizing antibodies and protects against lethal Nipah virus infection. *NPJ Vaccines* **2024**, *9*, 158. https://doi.org/10.1038/s41541-024-00954-5.
82. Aguilar, H.C.; Matreyek, K.A.; Choi, D.Y.; Filone, C.M.; Young, S.; Lee, B. Polybasic KKR motif in the cytoplasmic tail of Nipah virus fusion protein modulates membrane fusion by inside-out signaling. *J. Virol.* **2007**, *81*, 4520–4532. https://doi.org/10.1128/jvi.02205-06.
83. Avanzato, V.A.; Oguntuyo, K.Y.; Escalera-Zamudio, M.; Gutierrez, B.; Golden, M.; Kosakovsky Pond, S.L.; Pryce, R.; Walter, T.S.; Seow, J.; Doores, K.J.; et al. A structural basis for antibody-mediated neutralization of Nipah virus reveals a site of vulnerability at the fusion glycoprotein apex. *Proc. Natl. Acad. Sci. USA* **2019**, *116*, 25057–25067. https://doi.org/10.1073/pnas.1912503116.
84. Dang, H.V.; Cross, R.W.; Borisevich, V.; Bornholdt, Z.A.; West, B.R.; Chan, Y.P.; Mire, C.E.; Da Silva, S.C.; Dimitrov, A.S.; Yan, L.; et al. Broadly neutralizing antibody cocktails targeting Nipah virus and Hendra virus fusion glycoproteins. *Nat. Struct. Mol. Biol.* **2021**, *28*, 426–434. https://doi.org/10.1038/s41594-021-00584-8.
85. Byrne, P.O.; Fisher, B.E.; Ambrozak, D.R.; Blade, E.G.; Tsybovsky, Y.; Graham, B.S.; McLellan, J.S.; Loomis, R.J. Structural basis for antibody recognition of vulnerable epitopes on Nipah virus F protein. *Nat. Commun.* **2023**, *14*, 1494. https://doi.org/10.1038/s41467-023-36995-y.
86. Chan, Y.P.; Lu, M.; Dutta, S.; Yan, L.; Barr, J.; Flora, M.; Feng, Y.R.; Xu, K.; Nikolov, D.B.; Wang, L.F.; et al. Biochemical, conformational, and immunogenic analysis of soluble trimeric forms of henipavirus fusion glycoproteins. *J. Virol.* **2012**, *86*, 11457–11471. https://doi.org/10.1128/jvi.01318-12.
87. Dang, H.V.; Chan, Y.P.; Park, Y.J.; Snijder, J.; Da Silva, S.C.; Vu, B.; Yan, L.; Feng, Y.R.; Rockx, B.; Geisbert, T.W.; et al. An antibody against the F glycoprotein inhibits Nipah and Hendra virus infections. *Nat. Struct. Mol. Biol.* **2019**, *26*, 980–987. https://doi.org/10.1038/s41594-019-0308-9.
88. Loomis, R.J.; Stewart-Jones, G.B.E.; Tsybovsky, Y.; Caringal, R.T.; Morabito, K.M.; McLellan, J.S.; Chamberlain, A.L.; Nugent, S.T.; Hutchinson, G.B.; Kueltzo, L.A.; et al. Structure-Based Design of Nipah Virus Vaccines: A Generalizable Approach to Paramyxovirus Immunogen Development. *Front. Immunol.* **2020**, *11*, 842. https://doi.org/10.3389/fimmu.2020.00842.
89. Pigeaud, D.D.; Geisbert, T.W.; Woolsey, C. Animal Models for Henipavirus Research. *Viruses* **2023**, *15*, 1980. https://doi.org/10.3390/v15101980.
90. Findlay-Wilson, S.; Flett, L.; Salguero, F.J.; Ruedas-Torres, I.; Fotheringham, S.; Easterbrook, L.; Graham, V.; Dowall, S. Establishment of a Nipah Virus Disease Model in Hamsters, including a Comparison of Intranasal and Intraperitoneal Routes of Challenge. *Pathogens* **2023**, *12*, 976. https://doi.org/10.3390/pathogens12080976.
91. Geisbert, T.W.; Feldmann, H.; Broder, C.C. Animal challenge models of henipavirus infection and pathogenesis. *Henipavirus Ecol. Mol. Virol. Pathog.* **2012**, *359*, 153–177. https://doi.org/10.1007/82_2012_208.
92. Diederich, S.; Babiuk, S.; Boshra, H. A Survey of Henipavirus Tropism-Our Current Understanding from a Species/Organ and Cellular Level. *Viruses* **2023**, *15*, 2048. https://doi.org/10.3390/v15102048.
93. de Wit, E.; Munster, V.J. Animal models of disease shed light on Nipah virus pathogenesis and transmission. *J. Pathol.* **2015**, *235*, 196–205. https://doi.org/10.1002/path.4444.
94. Satterfield, B.A.; Cross, R.W.; Fenton, K.A.; Borisevich, V.; Agans, K.N.; Deer, D.J.; Graber, J.; Basler, C.F.; Geisbert, T.W.; Mire, C.E. Nipah Virus C and W Proteins Contribute to Respiratory Disease in Ferrets. *J. Virol.* **2016**, *90*, 6326–6343. https://doi.org/10.1128/jvi.00215-16.